Identifying the optimal nodes to enlarge the coupling range of pinning controllability

Ming-Yang Zhou, Rong-Qin Xu, Xiao-Yu Li, Hao Liao*

College of Computer Science and Software Engineering, Shenzhen University, Shenzhen 518060, P.R. China

Abstract

The Lyapunov exponent characterizes the convergence rate of a pinning system, which is widely evaluated by the ratio of the largest and the smallest eigenvalues of the laplacian relevant matrix. Here, we show that the eigenvalue ratio cannot precisely characterize the pinning controllability. Alternatively, we concern the strict candidate range of the coupling strength (coupling range), and address the problem of how to increase the coupling range. Larger coupling range means easier access to guarantee the pinning controllability in engineering, which is quite different from the widely discussed eigenvalue ratio metric. Besides, an efficient perturbation-based algorithm is proposed to identify the optimal pinning nodes to maximize the coupling range. Simulation results in real networks demonstrate the effectiveness of the proposed method.

Keywords: Complex network, pinning control, eigenratio, controller

1. Introduction

Many natural phenomena could be represented as the spreading dynamics in complex networks, including the spread of epidemics, rumor, advertisements and so on [1, 2]. Controlling the dynamics in complex networks is the ultimate proof of our understanding of these networks. Since a large number of real networks are hinged by a specific set of influential nodes [3, 4], the control is usually

*Corresponding author: Hao Liao
Email address: jamesliao520@gmail.com (Hao Liao*)

achieved by driving a small set of these influential nodes. Pinning control, which drives a networked system to a coherent state, provides convenient access to control the dynamics in complex networks [5, 6]. Thus, much energy was devoted to designing various strategies to enhance the pinning controllability, e.g., time delay, adaptive system, pulse feedback [7, 8, 9].

The problem of how to increase the pinning controllability only based on network structure has attracted much attention in complex networks [10, 11, 8]. One plausible approach is to choose topologically important nodes as the pinning nodes [12], for example, high-degree, betweenness, PageRank and so on [13, 14, 1]. Betweenness was once shown to have good performance in US airline and protein-protein interaction networks [15]. Yet, its performance fluctuates much across different networks [16]. In recent years, the field of complex networks has witnessed numerous fresh ranking methods that are capable of pinning control: Closeness, K-shell, Katz, LeaderRank, H-index, Non-backtracking matrix, eigenvector-based methods, etc [15, 14]. K-shell method performs well in choosing a single influential node, but fails in the case of multiple ones [17, 18]. Katz requires high time consumption when calculating the importance of nodes [14]. Non-backtracking matrix method treats edges as agents and conducts random walk on edges, which has simplified formalism in ref. [4] and performs well only in sparse networks [19]. For the particular pinning control problem, Amani et al. [20, 21, 22] proposed a perturbation method to choose influential nodes, which outperformed most state-of-the-art methods. Though the aforementioned heuristic methods largely enrich the selection of influential nodes, they cannot reach the optimal pinning control since choosing multiple influential nodes (influence maximization) is a NP-hard problem [4].

In the field of pinning control, the controllability is usually characterized by the ratio of the largest and the smallest eigenvalues of the laplacian relevant matrix, which is the widely used evaluation of the aforementioned methods. However, Zhou et al. [23] have recently shown that the ratio metric cannot precisely characterize the pinning controllability: Strictly speaking, the pinning controllability should be characterized by the Lyapunov exponent of a system,

and the classical ratio metric deviates from the Lyapunov exponent to some degree. Thus, the pinning controllability should be described from two perspectives: control speed (Lyapunov exponent) and coupling range. The former control speed characterizes the Lyapunov exponent, While the later coupling range characterizes the candidate range of coupling strength between nodes in which the network could be controlled. However, most previous works only focus on the control speed that is roughly evaluated by the ratio metric, neglecting the range of coupling strength (coupling range). Hence, we mainly concern the coupling range in the paper.

Here, we investigate the problem of how to choose optimal influential nodes to maximize the coupling range rather than the classical ratio metric. Based on the perturbation theory, we propose a novel method to characterize the influence of multiple pinning nodes on the coupling range. The analytical results show that the importance of nodes is determined by the eigenvectors corresponding to the largest and smallest eigenvalues of the laplacian relevant matrices. We then design an efficient algorithm to obtain the optimal pinning nodes that maximize the coupling range. Comparing with the state-of-the-art methods, our proposed method has the best coupling range and the best robustness in real networks. Besides, the simulation results also show that our method outperforms the state of the art methods in terms of the classical eigenratio metric.

The organization of the paper is as follows: In section 2, we describe the pinning control problem and the coupling range. In section 3, we introduce the coupling range and propose an efficient algorithm to choose influential pinning controllers. In section 4, the experimental results are presented. At last, the conclusion is given in section 5.

2. Preliminaries and definitions

Considering an undirected and unweighted network $G = (V, E)$ with $N = |V|$ nodes and $|E|$ edges, the state of each node is $\mathbf{x}_i = (x_{i1}, x_{i2}, ..., x_{in})^T \in R^n, \quad \forall i \in V$. Denote $A = (a_{ij})_{N\times N}$ being the adjacent matrix, $a_{ij} = 1$ if

$(i,j) \in E$; $a_{ij} = 0$ otherwise, and $L = (l_{ij})_{N\times N}$ being the laplacian matrix, where l_{ii} is the degree of node i and $l_{ij} = -a_{ij}(i \neq j)$. Neighboring nodes in the networks could exchange information and the network may arrive at a coherent state if the network satisfies some criteria [24, 25].

Assumption 1. All nodes follow identical nodal dynamics $f(x)$. Besides, there exists a stationary point (or trajectory) $\overline{\mathbf{x}} = (\overline{x}_1, \overline{x}_2, ..., \overline{x}_n)^T$ satisfying $\frac{d\overline{\mathbf{x}}}{dt} = f(\overline{\mathbf{x}})$.

In order to drive the system to the reference state $x_1(t) = x_2(t) = ... = x_N(t) = \overline{\mathbf{x}}$, we could simply inject identical feedback to a small fraction of nodes. Supposing that a set of nodes P are pinning nodes, we consider the dynamics of the linearly coupling system [26, 23]:

$$\begin{cases} \dfrac{d\mathbf{x}_i}{dt} = f(\mathbf{x}_i) - c\sum_{j=1}^{N} l_{ij} H\mathbf{x}_j, i \notin P, \\ \dfrac{d\mathbf{x}_i}{dt} = f(\mathbf{x}_i) - c\sum_{j=1}^{N} l_{ij} H\mathbf{x}_j - cdH(\mathbf{x}_i - \overline{\mathbf{x}}), i \in P. \end{cases} \tag{1}$$

where $f : R^n \to R^n$ is the individual systems' dynamical equation, $c > 0$ describes the coupling strength between agents, $H = (h_{ij})_{n\times n}$ is a matrix coupling different variables, and $d > 0$ is the feedback strength.

Theorem 1. For the local stabilization near the reference state $\overline{\mathbf{x}}$, the stabilization of Eq. 1 is equivalent to [27]:

$$\dot{\xi}_i = [Df + c\lambda_i H]\xi_i, i = 1, 2, .., N \tag{2}$$

where Df is the Jacobian function of f on $\overline{\mathbf{x}}$, ξ_i is a state variable linearly transferred from the node state x_i and λ_i is the eigenvalue of augmented laplacian matrix C $(0 > \lambda_1 \geq \lambda_2 \geq ... \geq \lambda_N)$. $C = -L - D$, $D = diag\{d_1, d_2, ..., d_N\}$, $d_i = d$ if i is a pinning node, $d_i = 0$ otherwise, i.e.,

$$C = \begin{bmatrix} -l_{11} - d_1 & -l_{12} & \cdots & -l_{1N} \\ -l_{21} & -l_{22} - d_2 & \cdots & -l_{2N} \\ \vdots & \vdots & \ddots & \vdots \\ -l_{N1} & -l_{N2} & \cdots & -l_{NN} - d_N \end{bmatrix}. \tag{3}$$

We now concern the generalized function of Eq. 2 as follows [27]:

$$\dot{y} = [Df + \alpha H]y. \tag{4}$$

Theorem 2. Stabilizing Eq. 4 requires the Lyapunov exponent of $[Df+\alpha H]$ being negative [28], i.e., the principle eigenvalue

$$\Lambda_{max}[Df + \alpha H] < 0. \tag{5}$$

A general stabilization condition for Eq. 4 is $\alpha \in (\alpha_2, \alpha_1) \quad (\alpha_2 < \alpha_1 < 0)$ [29], and we have $\alpha_2 < c\lambda_N \leq ... \leq c\lambda_1 < \alpha_1$.

Lemma 1: Equation 5 is roughly simplified as [29]:

$$R = \frac{\lambda_1}{\lambda_N} > \frac{\alpha_1}{\alpha_2}, \tag{6}$$

where R is the classical ratio metric to characterize pinning controllability of networks. Note that in some researches [30, 31], $\alpha_2 \to \infty$ is a particular case of Eq. 6 and the controllability is evaluated only by λ_1, we do not discuss the particular case in the following part. Increasing R is expected to have a large Lyapunov exponent.

3. Main results

3.1. The proposed coupling range for pinning controllability

Lemma 2: In order to better control the pinning controllability, the strict candidate range for the coupling strength c is

$$\omega = \frac{\alpha_2}{\lambda_N} - \frac{\alpha_1}{\lambda_1} > 0. \tag{7}$$

Remark 1. The eigenratio R (Eq. 6) cannot characterize the pinning controllability precisely. ω is a better metric to evaluate the pinning controllability.

An example of the difference between ω and R. We construct an artificial network with 18 nodes and 27 edges (See the network structure in Fig. 1(a)). The parameter settings are in section 4.3. We choose 6 pinning nodes using each baseline method (See section 4.2) and compare their corresponding ω in

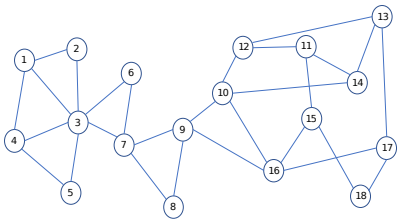

methods	pinning nodes	ω
PW	(1,5,8,11,13,17)	**0.248**
ESI	(1,2,3,4,5,7)	-2.293
Degree	(1,3,7,9,10,16)	-0.098
Betweenness	(3,7,9,10,15,16)	0.034
Closeness	(3,7,8,9,10,16)	-0.096
PageRank	(3,7,9,10,12,16)	0.040

(a) (b)

Figure 1: The schematic illustration of different methods to identify the optimal set of pinning nodes. The parameter settings are shown in section 4.3. (a) An artificial network consisting of 18 nodes and 27 edges. (b) The performance of different methods. The first column is the abbreviations of different methods (See section 4.2), the second column is the pinning nodes of different methods and the third column is the coupling range corresponding to different methods. $\omega > 0$ means possible coupling range and negative Lyapunov exponent in engineering, whereas $\omega < 0$ means positive Lyapunov exponent and hence the network cannot be controlled by the scheme, larger ω is better. Note that the bold PW index is the proposed perturbation of ω that achieves the largest coupling range.

Fig. 1(b). Fig. 1(b) shows that our method (PW index) has the highest coupling range. Whereas some R based methods (ESI, Degree and Closeness) have negative ω, meaning positive Lyapunov exponent $\Lambda_{max}[Df + \alpha H] > 0$. Thus, the network cannot be controlled by R based methods, and ω characterizes pinning controllability better than R.

Problem 1. Since most previous works investigate the pinning controllability only based on R in equation 6. The problem is how to identify influential nodes based on ω in equation 7.

3.2. Identifying the optimal pinning nodes

Theorem 3 (Single node): When we pin a single node in a network $G(N, E)$ (In Eq. 1), the optimal pinning node is determined by the perturbation of ω (PW) induced by adding a new pinning node i as:

$$PW(i) \approx \frac{1}{\lambda_1^2}[\alpha_2 R^2 (X_N^i)^2 - \alpha_1 (X_1^i)^2], \tag{8}$$

where R is the classical ratio metric, (X_N^i) and (X_1^i) are the $i-$th elements of eigenvectors X_N and X_1 ($|X_N| = |X_1| = 1$) that correspond to the smallest and largest eigenvalues of C.

Proof: Denoting that X_k is the eigenvector of the eigenvalue λ_i of the matrix C, $|X_k| = 1$. Supposing that we pin a new node i with feedback strength d_i, C becomes into $C' = C - \Delta D$, $\Delta D = diag\{0, ..., 0, d_i, 0, ..., 0\}$ with only one nonzero element d_i, the eigenvalue and the corresponding eigenvector of matrix C' become $\lambda'_k = \lambda_k + \Delta\lambda_k$ and $X'_k = X_k + \Delta X_k$ that satisfy:

$$(-L - D - \Delta D)(X_k + \Delta X_k) = (\lambda_k + \Delta\lambda_k)(X_k + \Delta X_k). \tag{9}$$

We can left-multiply Eq. 9 by X_k^T, after neglecting the second-order terms $\Delta D \Delta X_k$ and $\Delta\lambda_k \Delta X_k$, we arrive at [23]:

$$\frac{\partial \lambda_k}{\partial d_i} = -(X_k^i)^2, \tag{10}$$

where X_k^i is the $i-$th element of X_k.

The variation of ω induced by pinning the node i is

$$\frac{d\omega}{dd_i} = \frac{\alpha_1 \frac{\lambda_1}{d_i}}{\lambda_1^2} - \frac{\alpha_2 \frac{d\lambda_N}{d_i}}{\lambda_N^2}, \quad i = 1, 2, ..., N. \tag{11}$$

Substituting Eq. 10 into Eq. 11, we have:

$$\begin{aligned} \frac{d\omega}{dd_i} &= \frac{1}{\lambda_1^2}(\alpha_1 \frac{d\lambda_1}{d_i} - \alpha_2 \frac{\lambda_1^2}{\lambda_N^2} \frac{d\lambda_N}{d_i}) \\ &= -\frac{1}{\lambda_1^2}[\alpha_1 (X_1^i)^2 - \alpha_2 R^2 (X_N^i)^2]. \end{aligned} \tag{12}$$

Note that in the scenario $\alpha_2 << \alpha_1 \approx 0$, $\frac{d\omega}{dd_i}$ is mainly determined by the second term of the right hand side of Eq. 12. However, in most cases, we cannot ignore

the contribution of the first term in practice. For the identical feedback strength d for all pinning nodes, we can approximately calculate Eq. 8 based on Eq. 12. Hence, a node with the largest PW index influences more on the coupling range.

Theorem 4 (Multiple node): When a small fraction of nodes $P = \{x_1, x_2, ..., x_v\}(v << N)$ are considered as the pinning nodes, the perturbation of ω is

$$PW(P) \approx -\frac{1}{\lambda_1^2}[\alpha_1 \sum_{i=1}^{v} (X_1^i)^2 - \alpha_2 R^2 \sum_{i=1}^{v} (X_N^i)^2]. \tag{13}$$

Proof: we calculate the perturbation of λ_k based on the aforementioned proof as:

$$\frac{\partial \lambda_k}{\partial d_P} = -\sum_{i=1}^{v} (X_k^i)^2. \tag{14}$$

Substituting Eq. 14 into Eq. 11, we obtain Eq. 13.

Remark 2. Generally speaking, the increase of ω is the sum contribution of each pinning nodes. Thus, we can choose influential pinning nodes based on the $PW(i)$. Note that choosing pinning nodes based on the descending order of $PW(i)$ is the optimal strategy to maximize ω. The order of $PW(i)$ is irrespective of the feedback strength d. The central issue of our method is to use the PW index to determine the optimal set P.

Algorithm 1. Our algorithm to calculate the optimal nodes to maximize ω is as follows:

(1) Calculate the manifold (α_2, α_1) that guarantees the Lyapunov exponent to be negative.

(2) Initialize the pinning nodes set $P = \emptyset$.

(3) Obtain the augmented laplacian matrix C and eigenvectors X_1 and X_N corresponding to λ_1 and λ_N of C.

(4) Calculate the PW index of every node, choose the node with the largest $PW(i)$ $(i \notin P)$, and then add node i to set P.

(5) Repeat step (3)–(4) until the size of pinning nodes $|P|$ is satisfied, $|P| \geq v$.

Moreover, the pseudo code to compute the set of optimal pinning nodes is shown in Algorithm 1.

Algorithm 1 *PW* Algorithm

Input: $G(V, E)$; $f(x)$; H; v

Output: P

Calculate (α_2, α_1) that guarantees $\Lambda_{max}[Df + \alpha H] < 0$
Initialize a set $P = \emptyset$
repeat
    $C = -L - D$
    Calculate X_1 and X_N that corresponds to λ_1 and λ_N of C
    $R = \lambda_1/\lambda_N$
    for $i = 1$ to n **do**
        $PW(i) = \frac{1}{\lambda_1^2}[\alpha_2 R^2 (X_1^i)^2 - \alpha_1 (X_N^i)^2]$
    end for
    Choose the node $m(m \notin P)$ with maximal $PW(i)$
    Add node m into P
until $|P| = v$
Return P

4. Simulation results

4.1. Data description

To verify the effectiveness of the proposed methods, we conduct our experiments in 6 real networks. The real networks include "Italy powergrid" [32], "Moreno" [33], "Roundworm"[34], "Maayan" [35], "Facebook" [36] and "Petster"[37]. "Italy powergrid" is an infrastructure network, where an edge and a node represent a power supply line and a generator (or transformator, substation) respectively. "Moreno" is a protein network contained in yeast. "Roundworm" is a protein network of the roundworm. A node and an edge in "Moreno" and "Roundworm" represent a protein and a metabolic interaction

Network	N	E	H	r	$< C >$	$< d >$
Italy powergrid	68	93	1.175	-0.036	0.022	6.701
Moreno	1458	1948	2.667	-0.210	0.010	6.812
Maayan	1226	2408	1.873	-0.015	0.012	5.929
Facebook	744	30023	1.633	0.503	0.559	2.558
Roundworm	453	2025	4.485	-0.226	0.098	2.664
Petster	706	10064	1.549	0.035	0.400	2.737

TABLE II: Structural properties of the different networks. Structural properties include network size (N), link number (E), degree heterogeneity ($H =< k^2 > / < k >^2$), degree assortativity r, average cluster coefficient $< C >$ and average shortest-path length $< d >$.

between two proteins respectively. "Maayan" network is constructed from the USA's NFDC (National Flight Data Center). A node represents an airport or a service center and edges are created from preferred routes recommended by the NFDC. "Facebook" is a social network, where a node is a user and an edge represents a friendship between users. "Petster" is also a social network, which contains friendships and family links between users. Note that we treat all the networks unweighted and undirected and have no self-loops for convenience.

4.2. Baseline methods

We compare our method with five approaches: (i) degree centrality, (ii) betweenness centrality, (iii) closeness centrality, (iv) PageRank and (v) ESI index [38, 39, 40, 20]. Degree centrality of a node is defined as the number of links incident upon the node. Betweenness centrality of a node calculates how many times the node is acted as a bridge along the shortest path between two nodes. Closeness centrality of a node quantifies the average length of the shortest path between the node and all other nodes in the graph. A node with higher closeness centrality indicates the closer distance that the node has to other nodes. PageRank method is famous for ranking the web pages by Google,

which can be slightly simplified in undirected networks as [40]:

$$R(u) = \beta \sum_{v \in B_u} \frac{R(v)}{|B_u|},$$

where u and v are web pages, β is a normalization factor and B_u is the set of neighboring pages of u. It's widely accepted that the web page with higher PageRank index is more likely to be checked out by random surfer. ESI index is derived from the variation of the classic ratio metric R, which is defined as [20]:

$$ESI(i) = (X_N^i)^2,$$

where X_N^i represents the ith element of X_N that corresponds to the largest eigenvalue of the laplacian matrix L. Amani et al. [40] propose that the node with the maximum ESI has the strongest influence on the ratio metric R.

4.3. Parameter settings

In Eq. 1, the $f(\mathbf{x}_i)$ could represent various nodal dynamics, including Rössler attractor, Lorenz attractor, Chen attractor and so on [41, 42, 43]. Without loss of generality, in the simulation, we utilize Rössler attractor as nodal dynamics that follows:

$$\begin{aligned} \dot{x}_{i1} &= -x_{i2} - x_{i3}, \\ \dot{x}_{i2} &= x_{i1} + a_1 x_{i2}, \\ \dot{x}_{i3} &= a_2 + x_{i3}(x_{i1} - a_3), \end{aligned} \tag{15}$$

where $\mathbf{x} = (x_{i1}, x_{i2}, x_{i3})^T$, and a_1, a_2 and a_3 are tunable parameters. We set $a_1 = 0.2$, $a_2 = 0.2$ and $a_3 = 5$ in the simulation. We can calculate one of the stationary points as $\overline{\mathbf{x}} = (0.008, -0.040, 0.040)^T$, and the manifold as $(\alpha_2, \alpha_1) = (-4.991, -0.192)$ (See Fig. 2). We argue that the results and conclusions are not limited to the particular nodal dynamics and particular parameter settings.

4.4. Experimental results

We first pin 25 nodes to control Italy powergrid network and track x_{i1} of 3 nodes' state (The nodes with the largest degree, middle degree and smallest

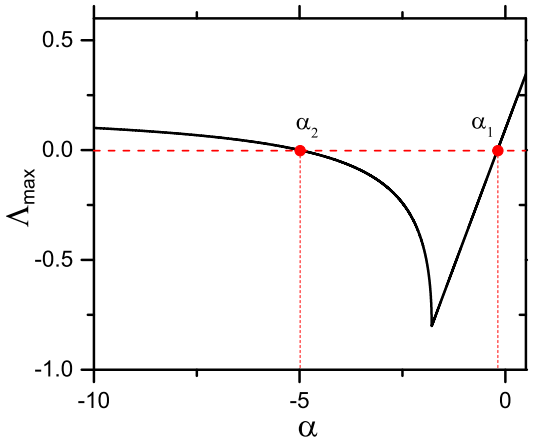

Figure 2: The largest eigenvalue Λ_{max} of matrix $[Df + \alpha H]$ as a function of α. In the figure, the manifold of the coupling range is $\alpha \in (-4.991, -0.192)$.

degree respectively). Here, we set $c = 0.48$ and $d = 5$. The initial states of each node follow the uniform distribution $0 \sim 1$. By controlling the nodes of PW in Fig. 3(a), the states of nodes converge to a stationary state, whereas in other panels, the states of nodes become chaos when we use other control strategies. Because only PW could choose nodes that guarantee $w > 0$, i.e., $\alpha_1/\lambda_1 < c < \alpha_2/\lambda_N$. Whereas for the other methods, $w < 0$ means positive Lyapunov exponent, and hence the network cannot be controlled under arbitrary coupling strength. The results show that only optimizing R cannot guarantee the control of the network. ω is a better metric to evaluate the pinning controllability than R.

In Fig. 4, we describe how the coupling range changes with the α_1 and α_2 when 10% nodes are considered as the pinning nodes in Moreno network. When $|\alpha_2| >> |\alpha_1|$, ω_{max} has large positive value, which means that the network can be well controlled. Note that in the case of $|\alpha_2| >> |\alpha_1|$, $PW(i)$ is largely determined by the principle eigenvector X_N based on Eq. 13, and thus the method reduces into the eigenvector-based method. In other cases, $PW(i)$ is influenced by both X_1 and X_N. With the increase of $|\alpha_1|$, ω_{max} decreases to a

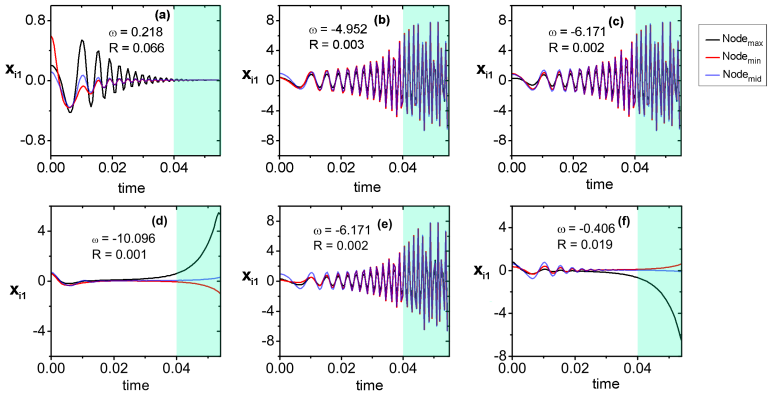

Figure 3: The state x_{i1} of three nodes (with largest degree, middle degree and smallest degree) as a function of time in Italy powergrid network when 25 nodes are controlled for different methods: (a) PW method. (b) Degree centrality. (c) Betweenness centrality. (d) ESI. (e) Closeness centrality. (f) PageRank. We use Rössler attractor as nodal dynamics (See section 4.3) and set the coupling strength $c = 0.48$ and feedback strength $d = 5$ in this simulation. Notice that only the proposed PW could achieve the control the pinning system in panel (a), whereas the other methods actually cannot guarantee the control of the dynamics.

negative value ($\omega_{max} < 0$), which means that the network cannot be controlled. In order to control a real network, we should set suitable parameters to guarantee large $|\alpha_2|$ and small $|\alpha_1|$. The results of the other networks are similar to Fig. 4 and are not shown here.

Figure 5 shows the coupling range ω as a function of the fraction $\theta = t/N$ of pinning nodes for different methods and different networks. In Fig. 5, the proposed method PW outperforms the other methods in most cases. Note that the performance of classical methods fluctuates much on different networks, for example, the PageRank method has a similar performance with the betweenness method in Figs. 5(b)(c), yet the performance of the two methods is completely different in Figs. 5(d)(e). Besides, the fluctuation exists widely for other baseline methods in other networks (not limited by the six networks in the paper).

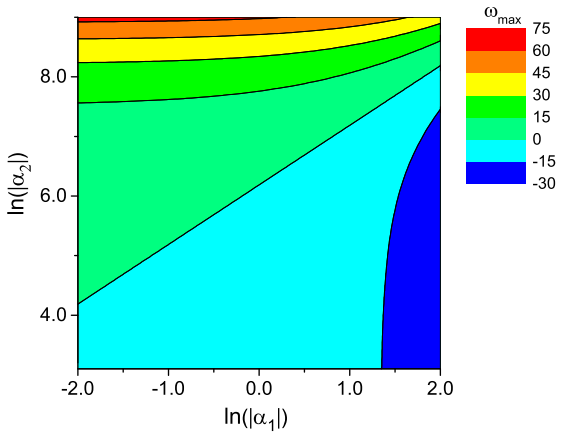

Figure 4: The ω_{max} as a function of α_1 and α_2 in Moreno network when 10% nodes are chosen as pinning nodes by the proposed method. The feedback strength d is the maximum degree of the nodes for networks.

Whereas our method still shows high robustness and performs well in most of real networks. Another interesting issue is that ESI index has the worst performance in Fig. 5. Because ESI index aims to maximize the ratio R rather than ω. Actually, the detection of influential nodes depends much on the dynamics being studied [44].

Moreover, we compare the performance of the chosen nodes based on the classical eigenratio R. In Fig. 6, PW method also outperforms other methods in most cases, which indicates that PW method helps increase the classic eigenratio R.

We also calculate the overlap of the pinning nodes sets between different approaches and PW method. The overlap is defined by the Hub Deoressed Index (HDI):

$$HDI_{PW\sim ESI} = \frac{|S_{PW} \cap S_{ESI}|}{max(|S_{PW}|, |S_{ESI}|)},$$

where S_{PW} and S_{ESI} are the sets of pinning nodes by PW and ESI methods. $|...|$ represents the size of the set. We calculate 20% pinning nodes for each

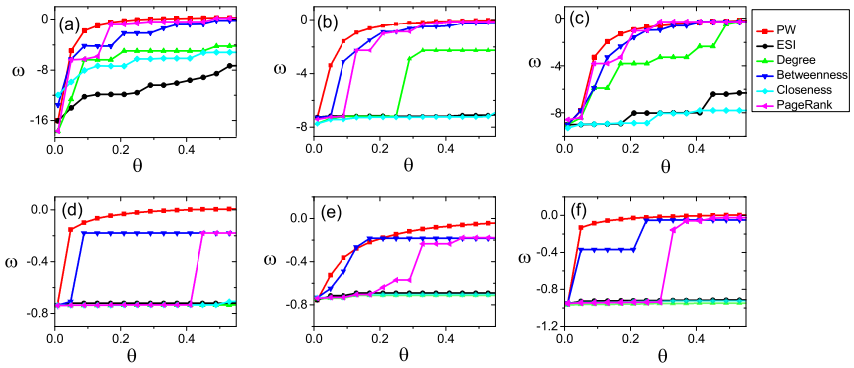

Figure 5: The coupling range ω as a function of the fraction $\theta = t/N$ of pinning nodes for different methods in different networks. The parameter settings are shown in section 4.3. Besides, the feedback strength d is the maximum degree of the nodes for networks. (a) Italy powergrid. (b) Maayan. (c) Moreno. (d) Facebook. (e) Roundworm. (f) Petster.

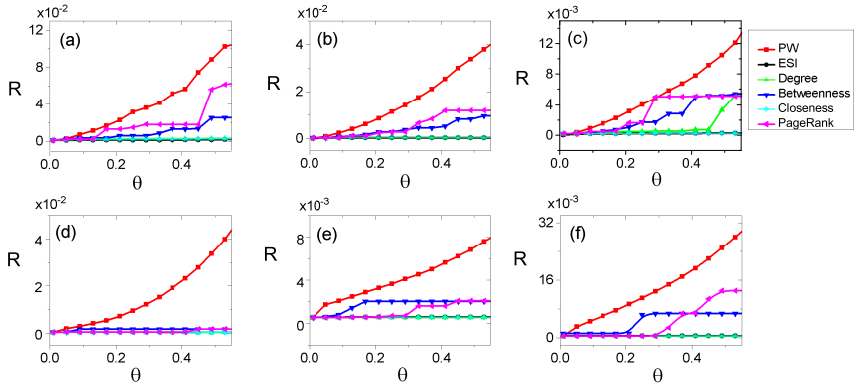

Figure 6: The eigenratio R as a function of the fraction $\theta = t/N$ of pinning nodes for different methods in different networks. The parameter settings are shown in section 4.3. Besides, the feedback strength d is the maximum degree of the nodes for networks. (a) Italy powergrid. (b) Maayan. (c) Moreno. (d) Facebook. (e) Roundworm. (f) Petster.

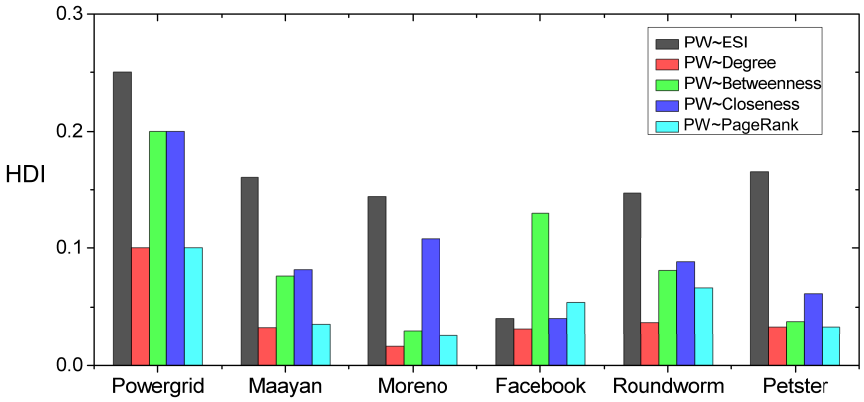

Figure 7: The pinning nodes intersection between PW method and the baseline methods. We calculate 30% pinning nodes for each method and compare the intersection. $PW \sim ESI$ (Degree, Betweenness, Closeness, PageRank) means the intersection of the optimal pinning nodes between PW and ESI (Degree, Betweenness, Closeness, PageRank). Besides, the feedback strength d is the maximum degree of the nodes for networks.

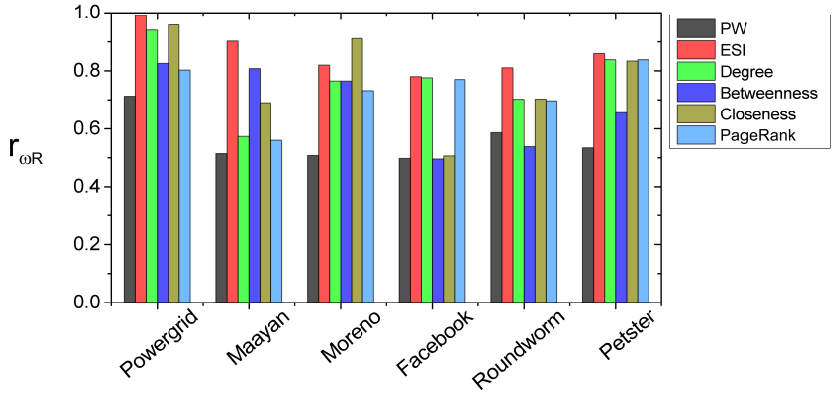

Figure 8: The Pearson correlation coefficient between the coupling range ω and eigenratio R. We set the coupling strength $c = 0.48$ and the feedback strength d being the maximum degree of the nodes. For each method and each network, we choose pinning nodes of the size 1% to 20% with size interval 1.5% and then calculate the corresponding vectors ω and R. After that, the pearson coefficient is obtained based on the vectors of ω and R.

method, and thus $|S_{PW}| = |S_{ESI}|$. It's clear that $0 \leq HDI \leq 1$ and larger HDI means different methods have more common pinning nodes.

Fig. 7 shows the overlap of the pinning nodes sets. In Fig. 7, the overlap of PW and other methods are small, which means that PW index can choose some particular nodes that may be neglected by other methods.

At last, in order to clarify the difference between the coupling range ω and classic eigenratio R, we calculate the Pearson correlation coefficient of the two parameters:

$$r_{\omega R} = \frac{\sum_{i=1}^{n}(\omega_i - \overline{\omega})(R_i - \overline{R})}{\sqrt{\sum_{i=1}^{n}(\omega_i - \overline{\omega})^2}\sqrt{\sum_{i=1}^{n}(R_i - \overline{R})^2}},$$

where $\overline{\omega}$ and $\overline{R}$ are the means of ω and R, $-1 \leq r_{\omega R} \leq 1$. $r = 1$ ($r = -1$) means totally positive (negative) linear correlation between ω and R and $r = 0$ means two independent variables.

In Fig. 8, ω and R have large correlation $r_{\omega R}$ ($r_{\omega R} > 0.5$) on the whole. However, for the pinning nodes of maximal ω (PW), the correlation $r_{\omega R} < 0.7$, meaning obvious difference between ω and R. Thus, optimizing ω cannot guarantee the optimum of R.

5. Conclusion

In conclusion, we address the coupling range and then use a perturbation-based method to maximize the coupling range. The proposed PW index could identify the optimal nodes to characterize the influence of multiple pinning nodes, irrespective of the classical ratio metric. We then propose an efficient algorithm to calculate PW and obtain the optimal influential nodes. Simulations in real networks demonstrate that our method outperforms other heuristic approaches in terms of both accuracy and robustness. Our research provides a deep understanding of pinning control in complex networks and can be used to design effective manmade systems as well.

6. acknowledgements

This work was jointly supported by the National Natural Science Foundation of China (Nos. 61703281, 11547040, 61803266, 61503140 and 61873171), the Ph.D. Start-Up Fund of Natural Science Foundation of Guangdong Province, China (Nos. 2017A030310374 and 2016A030313036), the Science and Technology Innovation Commission of Shenzhen (No. JCYJ201605 20162743717), Shenzhen Science and Technology Foundation (Nos. JCYJ20150529 164656096 and JCYJ20170302153955969), Guangdong Pre-national project (2014 GKXM054), Guangdong Province Key Laboratory of Popular High Performance Computers (2017B030314073), Foundation for Distinguished Young Talents in Higher Education of Guangdong (2015KONCX143), and the Young Teachers Start-up Fund of Natural Science Foundation of Shenzhen University.

Declaration of interest

The authors declare no competing interests.

Authors contribution

M.-Y.Z. and H.L. designed the research. R.-Q. X. and X.-Y. L. performed the experiments. M.-Y.Z., R.-Q. X., H. L. and X.-Y. L. analyzed the data and improved the method. M.-Y.Z. and X.-Y. L. wrote the manuscript and all authors have thoroughly proofread and revised the manuscript.

References

[1] L. Lü, D. Chen, X. Ren, Q. Zhang, Y. Zhang, T. Zhou, Vital nodes identification in complex networks, Phys. Rep. 650 (2016) 1–63.

[2] Z. Wang, M. Tang, S. Cai, Y. Liu, J. Zhou, D. Han, Self-awareness control effect of cooperative epidemics on complex networks, Chaos 29 (5) (2019) 053123.

[3] Y. Liu, J. Slotine, A. Barabási, Controllability of complex networks, nature 473 (7346) (2011) 167.

[4] F. Morone, H. Makse, Influence maximization in complex networks through optimal percolation, Nature 524 (7563) (2015) 65.

[5] W. Yang, Y. Wang, X. Wang, H. Shi, L. Ou, Optimal selection strategy for multi-agent system with single leader, in: 2012 IEEE 51st IEEE Conference on Decision and Control (CDC), IEEE, 2012, pp. 2767–2772.

[6] R. Olfati-Saber, Flocking for multi-agent dynamic systems: Algorithms and theory, Tech. rep., California Inst of Tech Pasadena control and dynamical systems (2004).

[7] D. Ding, Q. Han, Z. Wang, X. Ge, A survey on model-based distributed control and filtering for industrial cyber-physical systems, IEEE T. Ind. Inform. 15 (5) (2019) 2483–2499.

[8] X. Wang, H. Su, Pinning control of complex networked systems: A decade after and beyond, Annu. Rev. Control 38 (1) (2014) 103–111.

[9] G. Chen, Pinning control and synchronization on complex dynamical networks, Int. J. Control Autom. 12 (2) (2014) 221–230.

[10] Y. Han, W. Lu, T. Chen, C. Sun, Optimizing pinned nodes to maximize the convergence rate of multiagent systems with digraph topologies, Complexity 2019 (2019) 1–12.

[11] Y. Liu, A. Barabási, Control principles of complex systems, Rev. Mod. Phys. 88 (3) (2016) 035006.

[12] A. Amani, M. Jalili, X. Yu, L. Stone, Controllability of complex networks: Choosing the best driver set, Phys. Rev. E 98 (3) (2018) 030302.

[13] X. Jin, T. He, J. Xia, D. Wang, W. Guan, Adaptive general pinned synchronization of a class of disturbed complex networks, Communications in Nonlinear Science and Numerical Simulation 67 (2019) 658–669.

[14] H. Liao, M. Mariani, M. Medo, Y. Zhang, M. Zhou, Ranking in evolving complex networks, Phys. Rep. 689 (2017) 1–54.

[15] Z. Rong, X. Li, W. Lu, Pinning a complex network through the betweenness centrality strategy, in: 2009 IEEE International Symposium on Circuits and Systems, IEEE, 2009, pp. 1689–1692.

[16] J. Zhou, X. Yu, J. Lu, Node importance in controlled complex networks, IEEE T. Circuits-II 66 (3) (2018) 437–441.

[17] M. Kitsak, L. Gallos, S. Havlin, F. Liljeros, L. Muchnik, H. Stanley, H. Makse, Identification of influential spreaders in complex networks, Nat. phys. 6 (11) (2010) 888.

[18] X. Wu, W. Wei, L. Tang, J. Lu, J. Lü, Coreness and h-index for weighted networks, IEEE T. Circuits-I 66 (8) (2019) 3113–3122.

[19] S. Mugisha, H. Zhou, Identifying optimal targets of network attack by belief propagation, Phys. Rev. E 94 (1) (2016) 012305.

[20] A. Amani, M. Jalili, X. Yu, L. Stone, Finding the most influential nodes in pinning controllability of complex networks, IEEE T. Circuits-II 64 (6) (2017) 685–689.

[21] A. Amani, M. Jalili, X. Yu, L. Stone, A new metric to find the most vulnerable node in complex networks, in: 2018 IEEE International Symposium on Circuits and Systems (ISCAS), IEEE, 2018, pp. 1–5.

[22] M. Jalili, Effective augmentation of networked systems and enhancing pinning controllability, Physica A 500 (2018) 155–161.

[23] M. Zhou, X. Li, W. Xiong, H. Liao, The coupling strength versus convergence speed in pinning control, Nonlinear Dynam. (2019) 1–12.

[24] L. M. Pecora, Synchronization conditions and desynchronizing patterns in coupled limit-cycle and chaotic systems, Phys. rev. E 58 (1) (1998) 347.

[25] X. He, Z. He, X. Du, T. Chua, Adversarial personalized ranking for recommendation, in: The 41st International ACM SIGIR Conference on Research & Development in Information Retrieval, ACM, 2018, pp. 355–364.

[26] J. Zhou, J. Lu, J. Lü, Pinning adaptive synchronization of a general complex dynamical network, Automatica 44 (4) (2008) 996–1003.

[27] W. Yu, G. Chen, J. Lu, J. Kurths, Synchronization via pinning control on general complex networks, SIAM J. Control Optim. 51 (2) (2013) 1395–1416.

[28] X. Wang, G. Chen, Synchronization in scale-free dynamical networks: robustness and fragility, IEEE T. Circuits-I: Fundamental Theory and Applications 49 (1) (2002) 54–62.

[29] Z. Li, Z. Duan, G. Chen, L. Huang, Consensus of multiagent systems and synchronization of complex networks: A unified viewpoint, IEEE T. Circuits-I: Regular Papers 57 (1) (2009) 213–224.

[30] X. Wang, G. Chen, Pinning control of scale-free dynamical networks, Physica A 310 (3-4) (2002) 521–531.

[31] W. Yu, G. Chen, J. Lü, On pinning synchronization of complex dynamical networks, Automatica 45 (2) (2009) 429–435.

[32] A. Motter, S. Myers, M. Anghel, T. Nishikawa, Spontaneous synchrony in power-grid networks, Nat. Phys. 9 (3) (2013) 191.

[33] S. Coulomb, M. Bauer, D. Bernard, M. Marsolier-Kergoat, Gene essentiality and the topology of protein interaction networks, P. Roy. Soc. B-Biol. Sci. 272 (1573) (2005) 1721–1725.

[34] J. Duch, A. Arenas, Community detection in complex networks using extremal optimization, Phys. Rev. E 72 (2) (2005) 027104.

[35] Air traffic control network dataset – KONECT (Apr. 2017).
URL `http://konect.uni-koblenz.de/networks/maayan-faa`

[36] B. Viswanath, A. Mislove, M. Cha, K. Gummadi, On the evolution of user interaction in Facebook, in: Proc. Workshop on Online Social Networks, 2009, pp. 37–42.

[37] Hamsterster full network dataset – KONECT (Apr. 2017).
URL http://konect.uni-koblenz.de/networks/petster-hamster

[38] T. Opsahl, F. Agneessens, J. Skvoretz, Node centrality in weighted networks: Generalizing degree and shortest paths, Social networks 32 (3) (2010) 245–251.

[39] U. Brandes, A faster algorithm for betweenness centrality, J. Math. Sociol. 25 (2) (2001) 163–177.

[40] L. Page, S. Brin, R. Motwani, T. Winograd, The pagerank citation ranking: Bringing order to the web., Tech. rep., Stanford InfoLab (1999).

[41] O. E. Rössler, An equation for continuous chaos, Phys. Lett. A 57 (5) (1976) 397–398.

[42] I. Stewart, Mathematics: The lorenz attractor exists, Nature 406 (6799) (2000) 948.

[43] G. Chen, T. Ueta, Yet another chaotic attractor, Int. J. Bifurcat. Chaos 9 (07) (1999) 1465–1466.

[44] G. F. De Arruda, A. L. Barbieri, P. M. Rodríguez, F. A. Rodrigues, Y. Moreno, L. da Fontoura Costa, Role of centrality for the identification of influential spreaders in complex networks, Phys. Rev. E 90 (3) (2014) 032812.